XMM-NEWTON SPECTROSCOPY OF BRIGHT ULX SOURCES IN THE ANTENNAE GALAXIES (NGC 4038/4039)

J. M. MILLER[1,2], A. ZEZAS[1], G. FABBIANO[1], F. SCHWEIZER[3]

Subject headings: galaxies: individual (NGC 4038/4039) – Black hole physics – X-rays:galaxies – galaxies: stars

Draft version February 27, 2003

ABSTRACT

We report the results of spectral fits to bright ultra-luminous X-ray sources (ULXs) in the Antennae galaxies (NGC 4038/4039) obtained through a 41 ksec observation with *XMM-Newton*. Although emission regions are not resolved as well as in prior *Chandra* observations, at least four ULXs (X-11, X-16, X-37, and X-44 in the Zezas & Fabbiano scheme) are sufficiently bright and well-separated with *XMM-Newton* that reliable extractions and spectral analyses are possible. Fits to the source spectra with only the multi-color disk blackbody model give high disk color temperatures ($kT = 1.0-1.7$ keV); however, none of the spectra are acceptably fit by this model. Source X-37 is not well-fitted by *any* single component model. Fits with a model consisting of multi-color disk blackbody and power-law components may reveal a cool accretion disk ($kT = 0.13 \pm 0.02$ keV). Interestingly, when the multi-color disk blackbody plus power-law model is fit to all four ULXs, low temperatures are obtained for each ($kT = 0.11-0.21$ keV); however, only in X-37 is the cool disk component required. This suggests a parallel to recent spectral fits to the ULXs in NGC 1313, NGC 5408, and M74, in which soft components consistent with cool accretion disks may signal intermediate-mass black holes. The large number of ULX sources in the Antennae, however, suggests that many may be stellar-mass black holes, perhaps with emission focused along our line of sight as suggested previously.

1. INTRODUCTION

ULXs are off-nuclear point-like X-ray sources in nearby normal galaxies (Fabbiano & Trinchieri 1987, Fabbiano 1989). The X-ray flux variability observed in many ULXs (see, e.g., La Parola et al. 2001, Kubota et al. 2001) signifies that the class is likely dominated by accreting compact objects. The high luminosities measured from ULXs by definition exceeds the Eddington luminosity for an neutron star accreting isotropically; many exceed (sometimes by a factor of 10 or more) the Eddington luminosity expected for a 10 $M_{\odot}$ black hole.

Theoretical models for ULXs suggest that these sources may be stellar-mass sources with relativistically-beamed emission (Koerding, Falcke, & Markoff 2002), stellar-mass sources with anisotropic emission (King et al. 2001), or intermediate-mass black holes (IMBHs). Observations with *Chandra* and *XMM-Newton* — and especially multi-wavelength observing schemes — are beginning to reveal that no single model for ULXs may describe the entire class. Rather, the class may include examples of each possibility described above. NGC 5408 X-1 may be an example of a stellar mass source with relativistically-beamed emission (Kaaret et al. 2003); it is also possible that the spectrum can be described in part with a cool disk, which would indicate an IMBH. Many of the ULXs in the Antennae (there are 9 sources with $L_X \geq 10^{39}$ erg/s for a distance of 19 Mpc; Fabbiano, Zezas, & Murray 2001) may be stellar-mass sources with anisotropic emission. Finally, sources with high luminosities but low disk temperatures may be IMBHs; NGC 1313 X-1 and X-2 (Miller et al. 2003) and M74 X-1 (Krauss et al. 2003) may be examples.

At present, the anisotropic emission model (King et al. 2001) may be the most compelling description for a majority of ULXs. It is motivated in part by the unusually large number of ULXs resolved in the Antennae with *Chandra*. However, it may not be able to describe sources at the highest end of the ULX luminosity distribution (e.g., the sources with cool accretion disks mentioned above; see also Strohmayer & Mushotzky 2003). The high effective area of *XMM-Newton* allows observers to obtain high-quality medium-resolution X-ray spectra in relatively short exposure times. The spatial resolution of *XMM-Newton* is approximately five times more coarse than that of *Chandra*, but robust spectra can only be obtained from the brightest sources in targets with crowded fields like the Antennae.

Our *XMM-Newton* observation of the Antennae, then, is particularly well-suited to testing the anisotropic emission model with X-ray spectroscopy of the most luminous and well-separated ULXs. The procedure used to reduce our data and extract spectra is described in Section 2. In Section 3, we present the results of fitting simple spectral models to four bright ULXs. Finally, in Section 4, we discuss our results and their impact on our understanding of ULXs within the context of models for their nature and anomalous luminosity.

2. DATA REDUCTION AND ANALYSIS

The Antennae (NGC 4038/4039) were observed with *XMM-Newton* for 40.9 ksec on 8 January 2002, starting at 22:03:37 (UT). We used only the EPIC data for this analysis. The EPIC MOS-1 and MOS-2 cameras were operated in "PrimeFullWindow" mode and the EPIC-pn camera was operated in "PrimeFullWindowExtended" mode with the "medium" optical

[1]Harvard-Smithsonian Center for Astrophysics, 60 Garden Street, Cambridge, MA 02138, jmmiller@head-cfa.harvard.edu
[2]National Science Foundation Astronomy and Astrophysics Fellow
[3]Carnegie Observatories, 813 Santa Barbara St., Pasadena, CA 91101-1292

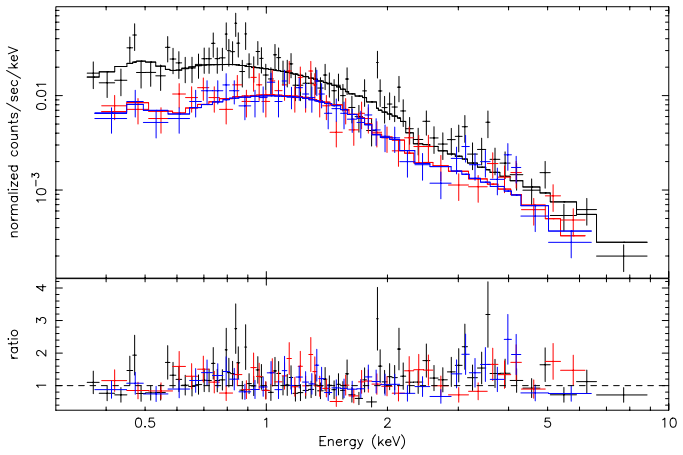

FIG. 1.— The pn (black), MOS-1 (red), and MOS-2 (blue) spectra of X-11 fit with a simple power-law model (see Table 1).

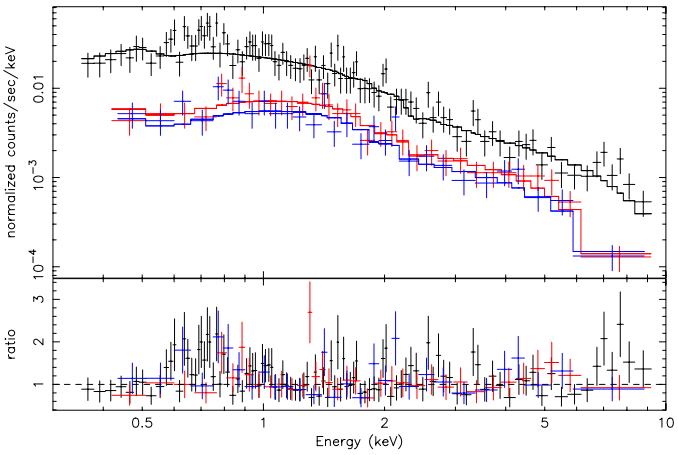

FIG. 2.— The pn (black), MOS-1 (red), and MOS-2 (blue) spectra of X-16 fit with a simple power-law model (see Table 1).

blocking filter in place. The *XMM-Newton* reduction and analysis suite SAS version 5.3.3 was used to filter the standard pipeline event lists, detect sources within the field, and make spectra and responses. After filtering against soft proton flares, the net "good time" for each camera was 22.6 ksec, 25.6 ksec, and 25.7 ksec for the pn, MOS-1, and MOS-2 cameras, respectively.

The ULX population in the Antennae is concentrated near the center of the interacting galaxies, which is a region with a dense source population. By relying upon the *Chandra* source detections, we determined that many sources are blended or too close to other bright sources to reliably extract a spectrum. Fortunately, at least four ULXs are well-separated from others, and/or bright enough that counts within a reasonable extraction region should be strongly dominated by the bright source. These sources are X-11, X-16, X-37, and X-44 (as numbered and identified by Zezas et al. 2002a).

We used circular regions centered on the known *Chandra* positions to extract source counts for these ULXs. For X-11, X-16, and X-44, source counts were extracted within a 12" radius; due to the proximity of a nearby source a 9" extraction radius was used for X-37. We did not extract background counts, as some of the background may be due to emission from nearby sources within this region. Observations with *Chandra* suggest that the background near to the ULXs we consider should be less than 1% of the source counts, however, and so should not significantly affect fits to the source spectra. The recipes described in the MPE "cookbook" were used to produce source spectra from the extracted counts. These parameters were chosen as follows: we set "FLAG=0" to reject events from bad pixels and events too close to the CCD chip edges; patterns 0-4 were selected for the pn camera, and patterns 0-12 for the MOS-1 and MOS-2 cameras; finally, the pn spectral channels were grouped by a factor of 5 and the MOS-1 and MOS-2 channels by a factor of 15. Response files for each camera were made using the SAS tools "rmfgen" and "arfgen". Prior to fitting, the spectra were grouped to require at least 10 counts per bin to ensure the validity of χ^2 statistics. Grouping to require more counts per bin did not significantly change the fit results.

The ULX lightcurves (in the 0.3–10.0 keV band, with 1.0 ksec bins) are well-described by a constant flux levels. We therefore considered only the time-averaged spectra from each ULX. Model spectra were fit to the data using XSPEC version 11.2 (Arnaud 1996). The pn, MOS-1, and MOS-2 spectra of each source were fit jointly, allowing an overall normalizing constant to account for small differences in the broad-band flux calibration of the cameras. Values obtained for the constant indicate that at the time of observation, the pn and MOS-1 flux calibrations differ by less than 5%. The MOS-2 flux calibration differed by less than 5% from the MOS-1 camera, but may have differed from the pn at the 10% level. Systematic errors were not added to the spectra prior to fitting. Models were fit to the EPIC spectra on the 0.3–10.0 keV band. Errors quoted in this work are at the 90% confidence level. Using the SAS tool "epatplot" and the HEASARC tool "PIMMS" we found that the effects of photon pile-up were negligible in this observation.

3. RESULTS

Lightcurves of the individual sources do not reveal strong variability on the timescale of this observation. We therefore made fits to the time-averaged spectra. Examination of the spectra did not reveal compelling evidence for emission or absorption lines; where a possible feature is seen in one spectrum (pn, MOS-1, or MOS-2), in each case there is no feature evident in the other spectra. This strongly suggests that any narrow deviations from a continuum spectrum are statistical fluctuations. We therefore restricted our modeling to continuum components. For each model, the "phabs" model in XSPEC was used to describe the equivalent neutral hydrogen column density along our line of sight. We fixed the lower bound of the equivalent neutral hydrogen column density to the Galactic value ($N_H = 4.0 \times 10^{20}$ cm^{-2}, Dickey & Lockman 1990). The results of fits with a number of simple models are listed in Table 1, and the results are described in detail below.

Prior fits to a number of ULX spectra (not sources within the Antennae) obtained with *ASCA* with the multicolor disk (MCD) blackbody model (Mitsuda et al. 1984) suggested that hot accretion disks may be a fundamental accretion flow structure in ULX sources (Makishima et al. 2000). Fits to X-11, X-16, X-37, and X-44 yielded high disk color temperatures ($1.0\text{keV} < kT < 1.7\text{keV}$), similar to prior *ASCA* results. However, this model does not yield an acceptable fit to any of the spectra. Other single-component models and two-component models are strongly preferred statistically (see below). This may suggest that X-11, X-16, X-37, and X-44 may be different from ULXs such as Dwingeloo X-1 (see Makishima et al. 2000). It is possible, however, that the apparent differences are partially due to the better sensitivity of *XMM-Newton*.

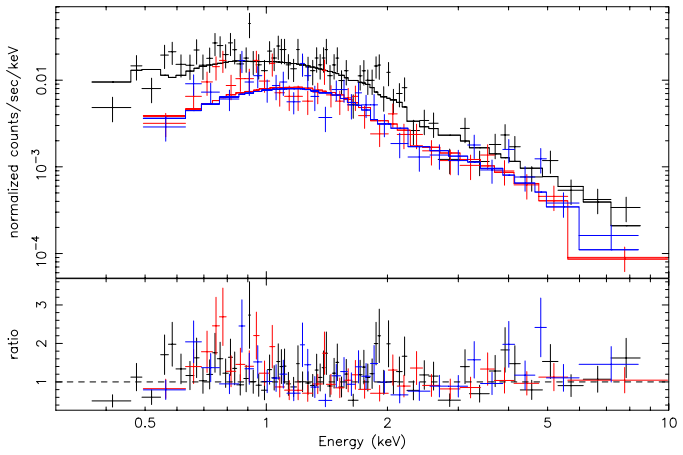

FIG. 3.— The pn (black), MOS-1 (red), and MOS-2 (blue) spectra of X-37 fit with a simple power-law model (see Table 1).

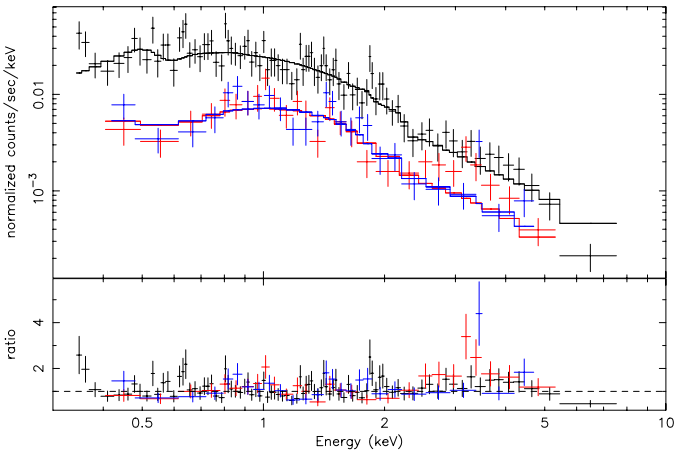

FIG. 4.— The pn (black), MOS-1 (red), and MOS-2 (blue) spectra of X-44 fit with a simple power-law model (see Table 1).

Significantly better fits are obtained when the spectra are fit with either a power-law or thermal Bremsstrahlung model. In accreting systems, most of the flux phenomenologically described as a power-law likely arises from the Compton-upscattering of relatively cool disk photons in an optically-thin corona (choose your favorite reference). A thermal Bremsstrahlung spectrum is consistent with expectations for an optically-thick, *geometrically* thick disk which may have a significant advective component (see, e.g., Ebisuzaki et al. 2001, Begelman 2002). Statistically acceptable fits to the spectra of X-11 and X-16 are obtained with either continuum model (see Table 1). The spectra of X-37 is not acceptably described with either model; a Bremsstrahlung model is a better description of the spectra from X-44 than a power-law model. The fits to X-11, X-16, X-37, and X-44 with a power-law model and associated data/model ratios are shown in Figures 1–4. The best-fit models for the spectra from each ULX are shown in Figure 5.

Finally, we considered a model consisting of MCD and power-law components. This simple model is often applied to stellar-mass black holes (STMBHs) in the Milky Way and Magellanic Clouds. This model permits an interesting comparison to recent ULX spectral results in which MCD color temperatures 5–10 times lower than commonly-measured in STMBHs may imply IMBHs as $T \sim M_{BH}^{-1/4}$ in the MCD model (Miller et al. 2003; see also Kaaret et al. 2003 and Krauss et al. 2003). While this model is not required to describe the spectra of X-11 or X-16, it provides a marginally better fit to X-44, and represents a statistically better fit to X-37 at the 3.5σ level of confidence based on an F-test. In each case, the color temperature obtained is consistent with a cool disk (the range of temperatures obtained is $0.11\text{keV} < kT < 0.21\text{keV}$). The power-law component represents a significant fraction of the 0.3–10.0 keV flux in this model. This may suggest that the gas in any optically-thin accretion flow geometry is very hot; if so, it is unlikely that the potentially cool thermal emission we have characterized with a disk model is actually due to local illumination of diffuse gas. This two-component model is the best description of the spectra of X-37; for this source we measure $kT = 0.13 \pm 0.02$ keV.

If color temperatures of $kT \sim 0.5-1.0$ keV may be taken as typical of STMBHs near to or above $L_X/L_{Edd.} \sim 0.1$, then color temperatures in the $kT \sim 0.11-0.21$ keV range may indicate black holes with masses in the range of $30\,M_\odot \leq M_{BH} \leq 6800\,M_\odot$ in these ULXs. The two-component MCD plus power-law model provides the best fit to X-37; for this source, black hole masses in the range $120M_\odot \leq M_{BH} \leq 7000M_\odot$ (90% confidence, including uncertainties in kT_{X-37} and STMBH disk color temperatures in the range $0.5\text{keV} \leq kT \leq 1.0\text{keV}$) may be suggested. It is worth noting, however, that the model used represents only a 3.5σ improvement to the spectra of X-37, far less than the 8σ improvement over single-component fits to NGC 1313 X-1 ($kT_{NGC1313X-1} = 0.15^{+0.02}_{-0.04}$ keV; Miller et al. 2003).

4. DISCUSSION

We have analyzed the *XMM-Newton*/EPIC spectra of four bright ULX sources (X-11, X-16, X-37, and X-44; as numbered by Zezas et al. 2002a). The spectra of two sources (X-16, X-11) can be well described by a single power-law ($\Gamma_{X-11} = 1.48$, $\Gamma_{X-16} = 1.9$). One of the other sources (X-44) is best described by a thermal bremsstrahlung model ($kT = 3.7$ *keV*) while the fourth source (X-37) requires two spectral components: a power-law ($\Gamma_{X-37} = 2.0$) and a MCD model ($kT_{in,X-37} = 0.15$ *keV*). Here we comment on the implications of these results for the nature of these sources and the general ULX population.

The coadded spectrum of the ULXs detected in the first *Chandra* observations of the Antennae was well represented by a composite MCD/power-law model with a temperature of 1.13 keV (Zezas et al. 2002b), while similar fits of the *XMM-Newton* spectra give temperatures in the $0.1-0.2$ keV range. This difference is most probably due to the fact that the *Chandra* results are for the coadded spectra of 18 sources, while here we study the detailed spectra of individual sources. In fact a comparison with the individual *Chandra* spectral fits for these sources (Zezas et al. 2002b) shows that the photon indices from the *Chandra* power-law fits are slightly flatter, but consistent within the 2 σ level, with those derived from the *XMM-Newton* fits. Similarly, the values of N_H from the *Chandra* fits are slightly higher than those derived from the *XMM-Newton* fits, but again consistent within the 2σ level. We note that no flux variability above the 3σ level has been detected between the two observations.

Both sources X-11 and X-16 have photon indices in the range observed in Galactic black-hole X-ray binaries (see, e.g., Tanaka & Lewin 1995). The non-detection of an MCD component might be due either to a low relative intensity compared to the power-law component, or because of its very low tempera-

ture (if the compact object is an IMBH). Very low disk temperatures and low disk fluxes are qualitatively consistent with the black hole low/hard state. Between its low/hard and high/soft states, Cygnus X-1 only varies by a factor of a few in soft X-rays (for a recent study, see Pottschmidt et al. 2002). This is similar to the level of variability observed in X-11 and X-16 (Fabbiano et al. 2003). In contrast, the flux measured from transient STMBHs can vary by several orders of magnitude between the low/hard and high/soft states.

If these ULX sources behave more like Cygnus X-1 than transient STMBHs, then it is possible that X-11 and X-16 are IMBHs in a low/hard state. However, it should be noted that these ULXs have been observed to vary in color-color diagrams based on *Chandra* data (Fabbiano et al. 2003) in a sense that is opposite to that seen in Cygnus X-1: X-11 and X-16 are spectrally harder when they are brighter. Finally, it is not clear that any state analogies are appropriate. Even in their brightest states, Cygnus X-1 and Galactic STMBHS are commonly observed at luminosities three and one orders of magnitude lower, respectively, than the ULXS analyzed in this work.

Finally, the MCD fit to the X-ray spectrum of source X-37 indicates that if it hosts an IMBH then its mass should be in the $120-7000\ M_{\odot}$ range. The comparison between its *Chandra* position and the positions of its nearby star-clusters shows that that there are no star-clusters down to $m_V = 23\ mag$ within a radius of 1.7" (Zezas et al. 2002), which translates to a physical distance of 156 pc ($d = 19.0$ Mpc). If this separation is due to a supernova kick to the system, and assuming that the X-ray binary becomes active in the end of the donor's main sequence lifetime, we can set an upper limit to its mass of $\sim 4\ M_{\odot}$ if the compact object has a mass of $270\ M_{\odot}$ (for a more massive BH the donor should be even smaller: e.g. A5 type for a $1000\ M_{\odot}$ IMBH). This corresponds to a star of spectral type B8 or later (e.g. Zezas & Fabbiano 2002). However, the large mass ratio between the IMBH and the donor makes this type of system prone to transient behavior. If this object is an IMBH, then there should be a much larger population of such systems throughout the Antennae (relatively few may be observed at any given moment, depending upon their duty cycles).

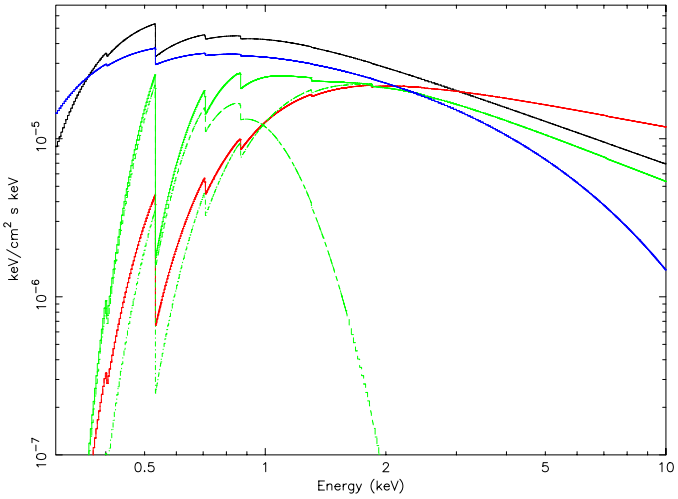

FIG. 5.— The best-fit models for each ULX source (see Table 1). In black: the power-law model for X-11. In red: the power-law model for X-16. In green, the MCD plus power-law model for X-37 (with disk and power-law components also shown in green). In red, the bremsstrahlung model fit to X-44. Clearly, the best-fit models for the ULX spectra we consider are significantly different; this may indicate different source types.

These results indicate that models for the ULX phenomenon based on a single source population may not be sufficient to describe the entire class. Instead, they suggest that ULXs could be a mixture of STMBHs and IMBHs. In the first case some type of anisotropic emission is required in order to explain their high luminosities (e.g., King et al. 2001).

J.M.M. acknowledges support from the NSF through its Astronomy and Astrophysics Fellowship Program. This work is based on observations obtained with *XMM-Newton*, an ESA mission with instruments and contributions directly funded by ESA Member States and the US (NASA). This work made use of the High Energy Astrophysics Archive Research Center (HEASARC), operated for NASA by GSFC.

REFERENCES

Arnaud, K. A., 1996, Astronomical Data Analysis Software and Systems V, eds. G. Jacoby and J. Barnes, p17, ASP Conf. Series vol. 101
Begelman, M. C., 2002, ApJ, 568, L97
Colbert, E. J. M., & Mushotzky, R. F., 1999, ApJ, 519, 89
Colbert, E. J., M., & Ptak, A. F., 2002, ApJS, 143, 25
Dickey, J. M., & Lockman, F. J., 1990, ARA& A, 28, 215
Ebisuzaki, T., et al., 2001, ApJ, 562, L19
Fabbiano, G., 1989, ARA & A, 28, 87
Fabbiano, G., & Trinchieri, G., 1987, ApJ, 315, 46
Fabbiano, G., Zezas, A., & Murray, S. S., 2001, ApJ, 554, 1035
Fabbiano, G., Zezas, A., King, A. R., Ponman, T. J., Rots, A., & Schweizer, F., 2003, ApJ, in press
Frank, J., King, A. R., & Raine, D. J., 2002, "Accretion Power in Astrophysics", (Cambridge Univ. Press: Cambridge)
Kaaret, P., Corbel, S., Prestwich, A. H., & Zezas, A., 2002, Science, in press
King, A. R., Davies, M. B., Ward, M. J., Fabbiano, G., & Elvis, M., 2001, ApJ, 552, L109
Kubota, A., Mizuno, T., Makishima, K., Fukazawa, Y., Kotoku, J., Ohnishi, T., & Tahiro, M., 2001, ApJ, 547, L119
La Parola, V., Peres, G., Fabbiano, G., Kim, D. W., Bocchino, F., 2001, ApJ, 556, 47
Madau, P., & Rees, M. J., 2001, ApJ, 551, L27
Makishima, K., et al., 2000, ApJ, 535, 632
Merloni, A. A., Fabian, A. C., & Ross, R. R., 2000, MNRAS, 313, 193
Miller, M. C., & Hamilton, D. P., 2002, MNRAS, 330, 232
Mitsuda, K., et al., 1984, PASJ, 36, 741
Pakull, M. W., & Mirioni, L., 2002, in the proceedings of the symposium "New Visions of the Universe in the XMM-Newton and Chandra Era", 26–30 November 2001, ESTEC, the Netherlands (astro-ph/0202488)
Pottschmidt, K., et al. 2002, A & A, subm., astro-ph/0202258
Shakura, N. I., & Sunyaev, R. A., 1973, A & A, 86, 121
Shimura, T., & Takahara, F., 1995, ApJ, 445, 780
Strohmayer, T. E., & Mushotzky, R. F., 2003, ApJL, in press
Watarai, K., Mizuno, T., & Mineshige, S., 2001, ApJ, 549, L77
Zezas, A., Fabbiano, G., Rots, A. H., & Murray, S. S., 2002a, ApJS, 142, 239
Zezas, A., Fabbiano, G., Rots, A. H., & Murray, S. S., 2002b, ApJ, 577, 710

TABLE 1

Spectral Fit Parameters

Model/Parameter	X-11	X-16	X-37	X-44
power-law				
N_H (10^{21} cm^{-2})	1.0 ± 0.2	0.4 ± 0.2	2.0 ± 0.3	1.3 ± 0.3
Γ	1.9 ± 0.1	1.48 ± 0.07	2.06 ± 0.09	2.2 ± 0.2
Norm. (10^{-5})	5.5 ± 0.7	3.6 ± 0.3	$5.3^{+0.9}_{-0.7}$	5 ± 1
$F_{0.3-10}$ (10^{-13} $erg\ cm^{-2}\ s^{-1}$)[a]	3.3 ± 0.4	2.9 ± 0.2	$2.5^{+0.4}_{-0.3}$	2.3 ± 0.5
χ^2/dof	162.6/160	140.0/164	163.0/129	162.6/139
MCD				
N_H (10^{21} cm^{-2})	0.4 ± 0.1	0.40 ± 0.02	0.4 ± 0.1	0.40 ± 0.03
kT (keV)	1.1 ± 0.1	$1.5^{+0.2}_{-0.1}$	1.2 ± 0.1	1.0 ± 0.1
Norm. (10^{-3})	7.0 ± 1.2	2.2 ± 0.7	$4.5^{+1.7}_{-1.2}$	9^{+2}_{-3}
χ^2/dof	245.8/160	258.8/164	220.2/129	194.8/139
Bremsstrahlung				
N_H (10^{21} cm^{-2})	0.4 ± 0.1	< 0.4	1.1 ± 0.2	$0.5^{+0.2}_{-0.1}$
kT (keV)	5.1 ± 0.8	12^{+6}_{-2}	4.5 ± 0.8	3.7 ± 0.5
Norm. (10^{-5})	6.0 ± 0.6	5.2 ± 0.4	5.1 ± 0.6	$4.9^{+0.7}_{-0.3}$
χ^2/dof	164.1/160	152.1/164	178.7/129	149.4/139
MCD + power-law				
N_H (10^{21} cm^{-2})	$3.0^{+0.8}_{-1.8}$	1.5 ± 1.0	5.6 ± 1.5	$1.4^{+2.0}_{-0.4}$
kT (keV)	0.15 ± 0.02	0.19 ± 0.05	0.13 ± 0.02	$0.15^{+0.02}_{-0.15}$
Norm.	50^{+10}_{-48}	5^{+1}_{-4}	250 ± 150	1^{+20}_{-1}
Γ	1.9 ± 0.2	1.4 ± 0.2	2.0 ± 0.2	$2.2^{+0.1}_{-0.4}$
Norm. (10^{-5})	$5.5^{+1.7}_{-1.0}$	$3.2^{+0.9}_{-0.7}$	5.4 ± 1.5	5.0 ± 1.0
χ^2/dof	153.2/158	131.5/162	143.8/127	162.2/137
F (10^{-13} $erg\ cm^{-2}\ s^{-1}$)[a]	$4.9^{+1.3}_{-2.5}$	$8.7^{+2.0}_{-5.2}$	$7.9^{+3.9}_{-2.8}$	$2.3^{+3.0}_{-0.5}$
$F_{power-law}/F_{total}$	0.61	0.33	0.33	0.77
$L_{0.3-10}$ (10^{40} erg/s)[b]	$2.1^{+0.7}_{-1.1}$	$3.7^{+0.9}_{-2.2}$	$3.4^{+1.7}_{-1.2}$	$1.0^{+1.3}_{-0.2}$

NOTE.—Results of fitting simple models to the EPIC spectra of four bright ULX sources in the Antennae galaxies. The XSPEC model "phabs"was used to measure the equivalent neutral hydrogen column density along the line of sight.

[a] The absorption-corrected or "unabsorbed" flux.

[b] The source luminosity in the 0.3–10.0 keV band for a distance of 19 Mpc.